# Origin of Landau oscillations observed in scanning tunneling spectroscopy on *n*-InAs(110)

M. Morgenstern,[1] D. Haude,[1] V. Gudmundsson,[2] Chr. Wittneven,[1] R. Dombrowski,[1] and R. Wiesendanger[1]
[1]*Institute of Applied Physics and Microstructure Research Center, Hamburg University, Jungiusstraße 11, D–20355 Hamburg, Germany*
[2]*Science Institute, University of Iceland, Dunhaga 3, IS-107 Reykjavik, Iceland*
(Received 11 February 2000)

The magnetic field induced oscillations in $dI/dV$ curves recorded with a low-temperature scanning tunneling microscope on *n*-InAs(110) are analyzed in detail. It is found that the previous interpretation of the oscillations as due to the Landau quantization of the bulk conduction band of InAs has to be reconsidered. While the distance between the maxima of the oscillation corresponds to the effective mass of the InAs conduction band, the energetic positions of the maxima depend on the individual tip and can only be understood if the tip induced quantum dot is taken into account. A comparison of measured quantities (spatial fluctuations of the Landau level energies and spin splittings) with Hartree-Fock calculations of the tip induced quantum dot reveals quantitative correspondence. From this comparison, we conclude that the tunneling experiment detects the $(m=0)$ states of different Landau and spin levels of the quantum dot, which are only marginally influenced by their resonant coupling to the bulk conduction band.

## I. INTRODUCTION

The detection of Landau quantization and spin splitting with lateral resolution provides insight into the complex interaction of electrons with potential inhomogeneities in a magnetic field. The lateral resolution appears to be crucial in semiconductor systems, since a number of intriguing experimental observations, such as, e.g., the quantum Hall effect, have been explained by rather local descriptions guided by localization phenomena in the residual potential disorder.[1] Scanning tunneling spectroscopy at low temperature is a technique that detects quantization energies with subnanometer lateral and sub-meV energy resolution[2] and is thus ideally suited to investigate local quantization phenomena in a magnetic field. Indeed, Landau quantization has been observed in experiments on *n*-InAs(110) and has been attributed to the Landau quantization of the bulk conduction band of the material.[3]

The aim of this paper is to clarify that this interpretation is not correct. A more careful analysis of the data reveals that neither the observed energetic positions of the Landau levels nor their intensity nor the observed spin splitting nor the influence of ionized dopants on the Landau levels can be explained within a model concentrating on the InAs bulk properties. Instead, another model has to be adopted: At positive sample voltages, the tunneling current proceeds from a nearly featureless tip density of states (DOS) to the quantized levels of the tip induced quantum dot.[4] Comparison of the experimental data with Hartree-Fock calculations of the quantum dot reveals good agreement. Thus we assume that the resonant coupling of the quantum dot levels to bulk bands is of minor importance. It broadens the levels, but does not significantly shift their energy.

## II. EXPERIMENT

The ultrahigh-vacuum low-temperature scanning tunneling microscopy (STM) apparatus is described in detail elsewhere.[5] The STM works down to 6 K and in magnetic fields up to 7 T perpendicular and 2 T parallel to the sample surface. The spectral resolution determined by the full width at half maximum (FWHM) of the smallest spectral features found in $dI/dV$ curves is 0.5 mV. This is in accordance with the expected thermal broadening of the Fermi level of the tip. Degenerate *n*-InAs ($N_D=2.0\times10^{16}/\mathrm{cm}^3$) is used. The dopant density and the degeneracy of the electron gas are checked by van der Pauw measurements at $T=4-300$ K. Hall and Shubnikov–de Haas measurements reveal that the electron gas remains degenerate up to 8 T and down to 4.2 K,[6] i.e., the carrier density is nearly independent of magnetic field. After *in situ* cleavage at a base pressure below $2\times10^{-8}$ Pa, the InAs sample is transferred into the STM and moved down into the cryostat. The procedure results in a clean InAs(110) surface with a STM-detectable adsorbate density of about $10^{-7}/\text{Å}^2$. The *ex situ* etched W tip is prepared *in situ* by applying voltage pulses up to 30 V and 10 ms between the tip and a W(110) sample and/or several hours of field emission at 150 V and 10 $\mu$A under feedback control. Topographic images and $dI/dV$ images are recorded in constant current mode with the voltage $V$ applied to the sample. The $dI/dV(V)$ curves are measured at fixed tip position with respect to the surface. The distance is fixed at a current $I_{\mathrm{stab}}$ and a voltage $U_{\mathrm{stab}}$ before the feedback is turned off. The $dI/dV(V)$ signal is recorded by lock-in technique ($f=1.5$ kHz, $V_{\mathrm{mod}}=1$ $\mathrm{mV_{rms}}$). Care has been taken to avoid spectral shifts induced by the finite time constant of the lock-in amplifier. Moreover, the voltage scale has been checked for each measurement by determining the zero current condition in the tunneling gap. Errors due to current offsets of the preamplifier (typically in the low picoamp range) are eliminated. Thus the total error in the absolute voltage scale is below 1 mV. All measurements are performed at $T=7\pm1$ K.

## III. RESULTS AND DISCUSSION

Figure 1 shows a set of $dI/dV(V)$ curves recorded with the same tip on the same sample position. The only param-

 

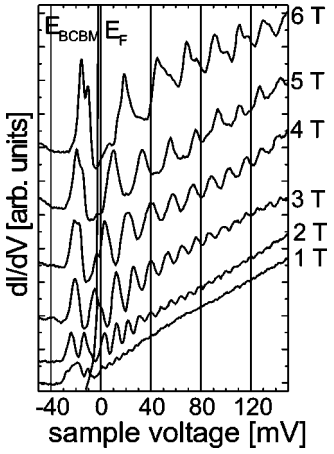


FIG. 1. $dI/dV(V)$ curves recorded with the identical tip on the same position of *n*-InAs(110) ($N_D=2.0\times10^{16}$ cm$^{-3}$) at different magnetic fields $B$ as indicated; $V_{\rm stab}=150$ mV, $I_{\rm stab}=500$ pA; $E_F$ marks the Fermi level and $E_{BCBM}$ the bulk conduction band minimum of the sample.

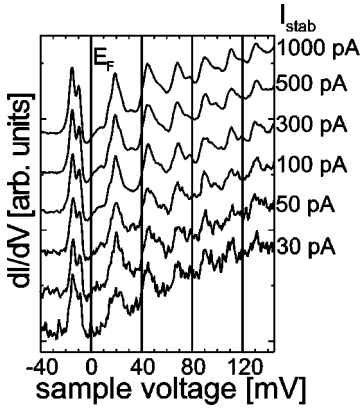


FIG. 2. $dI/dV(V)$ curves recorded with the identical tip on the same position of *n*-InAs(110) ($N_D=2.0\times10^{16}$ cm$^{-3}$) at $B=6$ T. The curves are stabilized at different $I_{\rm stab}$ as indicated; $V_{\rm stab}=150$ mV; $E_F$ marks the Fermi level.

eter varied is the magnetic field $B$ perpendicular to the sample surface. The Fermi level ($E_F$) as well as the bulk conduction band minimum ($E_{BCBM}$) of the InAs sample as obtained from calculations of the DOS of InAs with a carrier density of $2.0\times10^{16}$/cm$^3$ are marked.[7] $E_{BCBM}-E_F$ decreases with increasing $B$ due to the increasing DOS close to $E_{BCBM}$. The $dI/dV$ curves show distinct peaks below $E_{BCBM}$, which are caused by the tip induced quantum dot[4] (see below). Above $E_{BCBM}$, additional oscillations are observed. They increase in intensity and distance with increasing $B$. Identifying the voltage scale with the energy scale of the sample DOS,[2] one finds that the distance of the oscillation maxima $\Delta E$ corresponds to the effective mass $m_{\rm eff}(E)$ of InAs, i.e., $\Delta E(E)=\hbar eB/m_{\rm eff}(E)$ with $m_{\rm eff}(E)=0.023m_e[1+2(E-E_{BCBM})/E_{\rm gap}]$ ($\hbar$ is Planck's constant, $e$ the electron charge, $m_e$ the electron mass, $E_{\rm gap}=0.4$ eV the band gap of InAs).[3,8,9] The same magnetic field dependent peak distances reflecting $m_{\rm eff}(E)$ are found in all experiments. This experimental finding leads to the wrong conclusion that the *dI/dV* oscillations are caused by the Landau quantization of the bulk DOS of InAS (3).

However, the peak energies depend on the individual tip and do not correspond to the bulk DOS of InAs. The bulk DOS of InAs exhibits Landau and spin quantization in magnetic field and has a pole at $E_{BCBM}$.[7] This should result in a maximum in the $dI/dV$ curves at $E_{BCBM}$, which is not observed (Fig. 1). One easily deduces from the curves at 2 T, 5 T, and 6 T that broadening of the peaks caused by the finite lifetime of the electrons is not sufficient to explain the wrong peak positions. Moreover, energy shifts due to surface states can be excluded, since it is well known that InAs(110) exhibits flat band conditions up to the surface.[10]

A possible cause for an energy shift of the peaks in $dI/dV$ curves with respect to the DOS could be the usually assumed fact that the tunneling current is not sensitive to ($k_z=0$) states ($k_z$ is the electron wave vector perpendicular to the surface). Thus the tip could act as a $k_z$ filter. However, since $k_z$ is not influenced by the magnetic field, the peaks observed with a $k_z$ filter should be equidistant from $E_{BCBM}$ independent of $B$. This is not the case as shown in Fig. 1.

Another possible cause for energy shifts could be a local charging of the surface by the tunneling current, usually called spreading resistance.[11] It should result in a strong current dependence of the peak positions. Figure 2 shows $dI/dV$ curves measured with the same tip on the same surface position at $B=6$ T. $I_{\rm stab}$ and thereby the tunneling current is varied. A slight current dependent shift of about 1 meV is observed. It is attributed to the changing distance between sample and tip, which slightly changes the extension of the tip induced quantum dot.[8] However, this extremely small shift excludes an influence of spreading resistance on the peak energies.

Summarizing the above results, we state that the peaks in $dI/dV$ curves recorded in a magnetic field do not detect the Landau quantization of the unperturbed bulk DOS of InAs. Consequently, we have to consider the local perturbation of the sample by the electric field of the tip. In a previous publication,[4] we described this perturbation as a tip induced quantum dot. From the peaks in $dI/dV$ curves recorded at 0 T, we estimate the potential depth and the lateral extension of this quantum dot. For this, the measured peak energies are compared with Hartree calculations for different trial potentials. It is found that a Gaussian shape of the lateral extension of the quantum dot gives a reasonable description, i.e., the lateral extension can be described by a single parameter, the $\sigma$ width of the Gaussian. The potential of the quantum dot in the $z$ direction is modeled by solving the one-dimensional Poisson equation. The $z$ potential largely determines the energy of the lowest state. Since the potential depth of the quantum dot changes with applied voltage, the work function difference between sample and tip, $\Delta\Phi$, has to be used as the parameter to describe the $z$ potential. Thus the two parameters $\sigma$ and $\Delta\Phi$ completely determine the quantum dot shape. For W tips used on *n*-InAs(110), $\Delta\Phi$ turns out to vary between 70 meV and 400 meV, while $\sigma$ varies between 15 nm and 40 nm. Notice that the fitting procedure based on experimental data gives a good estimate of the potential shape of the dot, but neglects possible asymmetries of the quantum dot parallel to the surface.

It is obvious that the presence of the quantum dot changes the conditions of the tunneling experiment. Consequently, the energetic positions of the Landau oscillations should de-

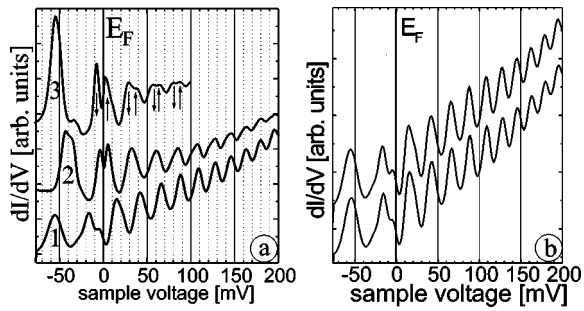


FIG. 3. $dI/dV(V)$ curves averaged from $100\times100$ curves recorded on a (200 nm $\times$ 200 nm) area at $B=6$ T. (a) Each curve is recorded with a different microtip: (1) $V_{\mathrm{stab}}=$ 200 mV, $I_{\mathrm{stab}}=450$ pA; (2) $V_{\mathrm{stab}}=200$ mV, $I_{\mathrm{stab}}=500$ pA; (3) $V_{\mathrm{stab}}=100$ mV, $I_{\mathrm{stab}}=500$ pA; arrows in curve 3 mark different spin levels. (b) Two averaged $dI/dV(V)$ curves recorded with the same microtip on different $(200\ \mathrm{nm})^2$ areas of the sample [averaging as in (a)]; $E_F$ marks the Fermi level.

pend on the actual microtip and the corresponding tip induced quantum dot. This is indeed the case, as demonstrated in Fig. 3(a). Three $dI/dV$ curves obtained with different microtips at $B=6$ T are shown. The three tips were prepared individually, resulting in different quantum dots as deduced from the different positions of the tip induced states (below $E_{BCBM}$). Since the three measurements are not performed on the same sample position, we used an averaging procedure to get rid of influences of the spatially fluctuating surface potential. Therefore we recorded a grid of $100\times100$ $dI/dV$ curves covering a $(200\ \mathrm{nm})^2$ area and plotted the average curve. To prove that the remaining potential fluctuations do not cause considerable peak shifts, Fig. 3(b) shows two averaged curves recorded with the same microtip on different $(200\ \mathrm{nm})^2$ areas. The remaining peak differences are below 1 meV, far smaller than the peak differences obtained with different microtips.

In addition, the top curve in Fig. 3(a) exhibits a splitting of the Landau oscillations. A similar splitting is partly observed with the other tips but only in single curves and not in the average curve. For example, in the data set from which the bottom curve of Fig. 3(a) was obtained, only 10% of the individual curves exhibit the splitting. Since the splitting is always twofold and of the order of the expected spin splitting of InAs (5.2 meV), it is attributed to spin splitting as indicated by the arrows on the top curve.

We have to draw the important conclusion that the Landau and spin quantization visible in $dI/dV$ curves strongly depends on the microtip. Since it is not reasonable to assume that the tip DOS results in peaks corresponding to the Landau and spin quantization of InAs, we consider the influence of the tip induced quantum dot as the remaining possible reason in more detail.

We determined the potential shape of the quantum dot as present during the measurement of the bottom curve of Fig. 3(a) ($\sigma=40$ nm, $\Delta\Phi=200$ meV) and performed unrestricted Hartree-Fock calculations of this quantum dot in a magnetic field. For technical reasons, we used periodic boundary conditions for a ($100\ \mathrm{nm}\times100$ nm) unit cell. In magnetic fields above 1.5 T the resulting energy bands $E(\mathbf{k})$ are flat, i.e., the quantum dots are decoupled and the states resemble those of an isolated dot. The individual states are classified by three

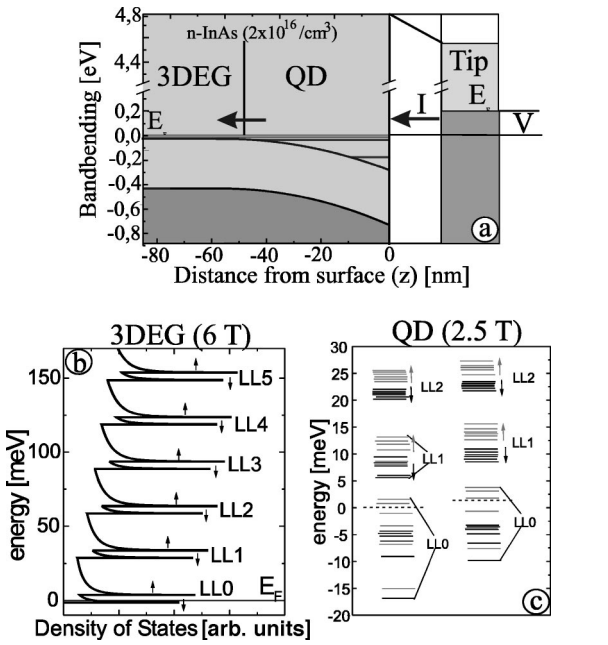


FIG. 4. (a) Sketch of the tunneling process at positive $V$: occupied levels are marked in dark gray, unoccupied levels are marked in light gray, the band gap of InAs is marked in very light gray, arrows mark the tunneling current $I$; QD is the tip induced quantum dot; 3DEG the three-dimensional electron gas. (b) Density of states of the 3DEG at $B=6$ T: LL$n$ and the arrows mark the different Landau and spin levels of the 3DEG, respectively. The smooth gray line includes the level broadening caused by the finite electron lifetime. (c) Level diagrams of the tip induced quantum dot at $B=2.5$ T: LL$n$ and the arrows are used as in (b); in addition spin up and spin down levels are drawn black and gray, respectively; the QD is calculated with the parameters $\Delta\Phi=200$ meV, $\sigma=40$ nm as obtained from the analysis of the tip used for the $dI/dV$ curve 1 in Fig. 3(a); right and left diagrams are calculated with and without a dopant in the center of the quantum dot, respectively.

quantum numbers $n$, $m$, and $s$ corresponding to the Landau quantization, the orbital momentum, and the spin.[12] The calculations were performed for several magnetic fields between 1.5 T and 3 T. To perform the calculations on a reasonable time scale, we had to restrict ourselves to $B\leqslant3$ T. However, from calculations performed at different magnetic fields and from our experience with previous Hartree-Fock calculations, we can assume that the trends scale up to 6 T.[13] All experimental data compared with Hartree-Fock calculations are measured with the corresponding microtip.

The computation of the quantum dot states allows us to sketch a more realistic picture of the tunneling experiment as shown in Fig. 4. A rather featureless DOS of the tip can be deduced from the flat $dI/dV$ curves observed at positive sample voltages and $B=0$ T. From this tip the electrons are injected into the quantum dot region (QD), which is resonantly coupled to the bulk conduction band (3DEG) of InAs. Decoupling the two regions of the sample in a gedanken experiment, we depict the corresponding DOS separately.

Figure 4(b) shows the bulk DOS at $B=6$ T, which is dominated by the Landau quantization calculated from $m_{\mathrm{eff}}(E)$ and the spin splitting resulting from $\Delta E_s=g\mu B$, with the gyromagnetic factor of InAs $g=14.8$ and Bohr's magneton $\mu$. $E_F$ is calculated by filling all electrons into the

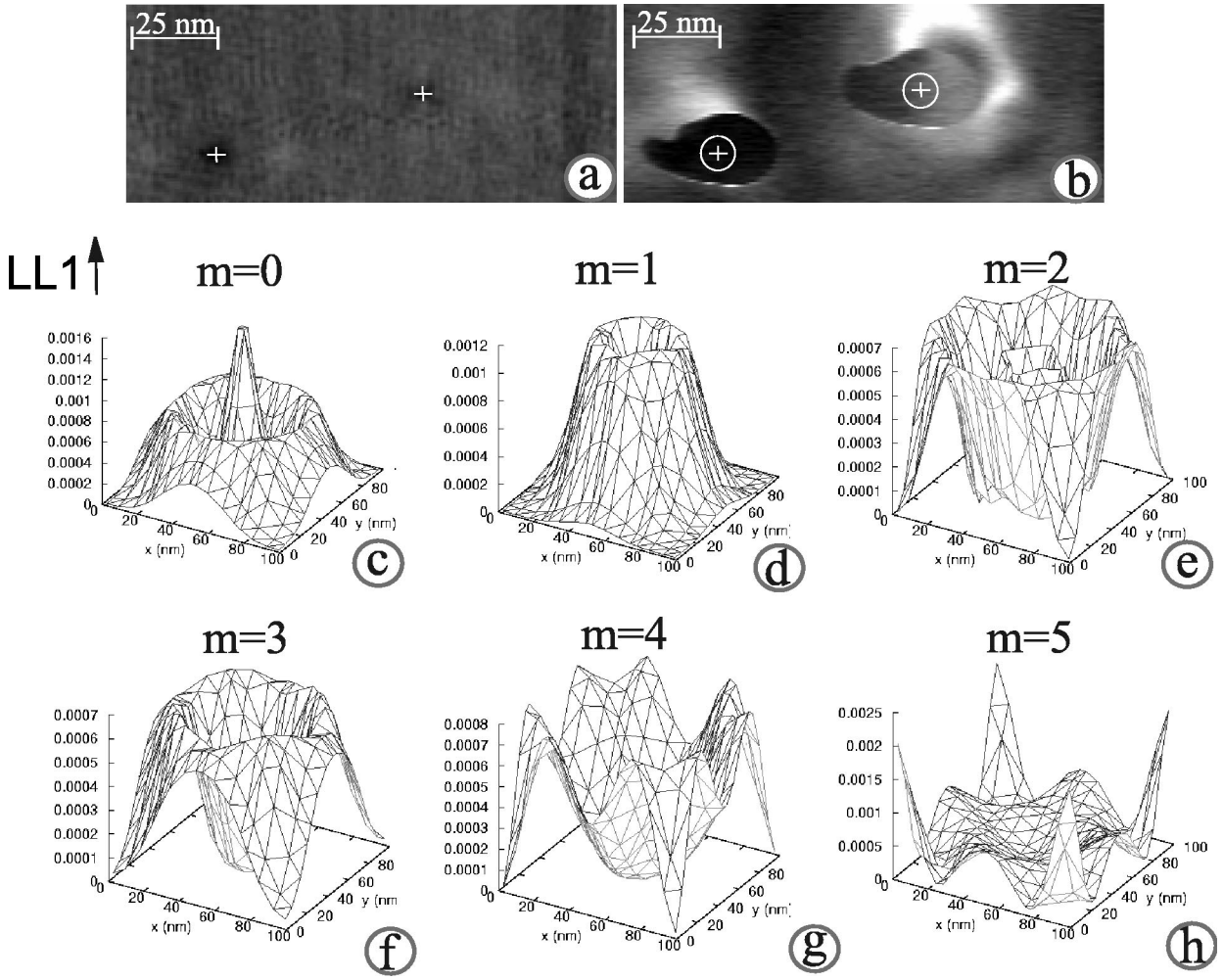


FIG. 5. (a) Constant current image of *n*-InAs(110) including two defects marked by crosses; $V=55$ mV, $I=500$ pA. (b) $dI/dV$ image recorded in parallel with (a); crosses mark the identical positions as in (a) and the rings mark the areas less than 5 nm away from each cross. (c)–(g) The wave functions of the LL1 spin up level of the quantum dot at $B=2.5$ T [corresponding to the energy levels shown in Fig. 4(c) right]; *m* marks the orbital momentum of each state.

resulting DOS. Since the finite electron lifetime leads to broadening of the energy levels, the real bulk DOS looks more like the curve shown as a gray line in Fig. 4(b). It is calculated by assuming a Lorentzian broadening of the DOS depicted in black (infinite electron lifetime). The electron lifetime used to calculate the gray line is taken from the resistivity of the sample at $B=0$ T assuming a Drude-model. Interestingly the oscillations of the ''real'' DOS (15% peak-to-peak with respect to the total DOS) are by far smaller than the oscillations observed in *dI/dV*-curves (up to 70% of the total *dI/dV*-signal). This again shows that the 3DEG DOS can not be responsible for the observed oscillations.

Figure 4(c) shows the quantum dot states as obtained from Hartree-Fock calculations. The two level schemes in Fig. 4(c) are calculated with the same quantum dot parameters, but in the left scheme an ionized dopant is added to the potential in the center of the quantum dot. First, one notices that the quantum dot states form bunches corresponding to different Landau numbers *n* and partly to different spin *s*. Second, the energetic distances between adjacent *n* bunches correspond exactly to the effective mass $m_{\mathrm{eff}}(E)$ of bulk InAs. Third, in agreement with the experimental results, the energetic positions of the bunches are different from the peaks in the bulk DOS; in particular, no bunch center is located close to 0 meV. All three results hold for all calculated magnetic fields and also for dots calculated with slightly different filling factors. So the experimental results can be explained by the Landau and spin quantization of the quantum dot without considering the influence of the bulk conduction band.

Let us assume for the moment that $dI/dV$ curves are sensitive only to the quantum dot states and ask what states are selected by the tunneling process. Atomic resolution is usually achieved, so the tunneling current is restricted to a sub-nm$^2$-area. Consequently, we couple only to a small part of the wave functions of the quantum dot states and the position of the tunneling region with respect to the dot will affect the measurement. Both the shape of the quantum dot and the position of the tunneling current can be determined when charging phenomena take place at small defects on the surface.[14]

Constant current images measure the position of the defects as marked by the crosses in Fig. 5(a). At the cross the tunneling region of the tip is exactly above the defect. On the other hand, a capacitive charging of the defect by the tip induced electric field takes place. If the electric field is suf-

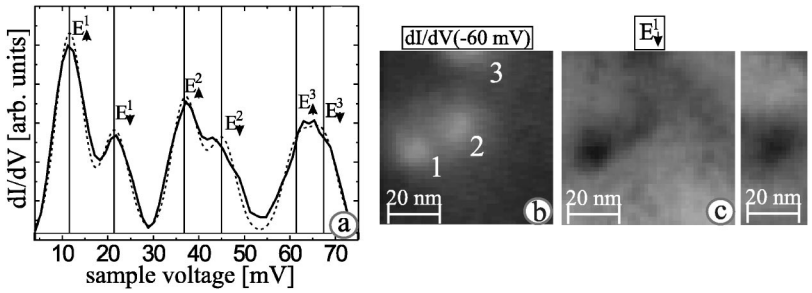


FIG. 6. (a) Single $dI/dV(V)$ curve (solid line), $B=6$ T, $V_{\mathrm{stab}}=200$ mV, $I_{\mathrm{stab}}=450$ pA, and corresponding fit using a Gaussian of width $\sigma=3.2$ meV for each peak (dashed line); the vertical lines labeled $E_s^n$ mark the resulting peak energies of different Landau levels $n$ and spin levels $s$. (b) $dI/dV$ map at $V=-60$ mV; bright areas labeled 1–3 correspond to dopants below the surface. (c) and (d) Maps of the peak energies $E_{\downarrow}^1$ and $E_{\uparrow}^1$ of the same area as depicted in (b); the peak energies are obtained from fits as shown in (a); notice the smooth shift of the peak energies around the dopants.

ficient to overcome the Coulomb blockade, the defect gets an additional negative charge, which repels the DOS in its environment and leads to a reduction in the $dI/dV$ signal. Indeed, we observe two dark areas appearing around the defects in Fig. 5(b). The borderlines of the dark areas mark the region of the same tip induced electric field sufficient to charge the defect. So, we directly measure the electric field of the tip. However, in contrast to the usual electrostatic experiments, we move the cause of the electric field (the tip) and not the probe (the defect). Hence, the point inversion of the borderline of the dark area corresponds to an equipotential line of the electrostatic tip. Since the equipotential lines directly induce the quantum dot, the dark areas mimic the shape of the quantum dot.

More importantly, the position of the tunneling current with respect to the quantum dot can be determined by comparing Figs. 5(a) and 5(b). Figure 5(a) marks the position of the tunneling current with respect to the defect and Fig. 5b the position of the quantum dot with respect to it. To guide the eye the position of the tunneling current is marked as a cross in both images. Obviously the tunneling current flows in the center of the quantum dot. To illustrate that it truly flows within 5 nm from the center of the dot, a circle with 5 nm radius is drawn around the cross in Fig. 5(b).

We conclude that only wave functions with a considerable weight in the inner 5 nm of the dot will be detected by $dI/dV$ curves. To select these states we use the Hartree-Fock calculations of a circular symmetric dot. Figures 5(c)–5(h) show a set of different $m$ states for Landau level $n=1$ and $s=\uparrow$ as obtained from the calculations. The $(n=1,s=\downarrow)$ states are identical. Only the $(m=0)$ state has a considerable intensity in the inner 5 nm of the dot. This is a general result holding for all Landau levels in all calculations performed in different magnetic fields. Consequently, we assume that the $(m=0)$ states will always dominate the signal in $dI/dV$ curves.

Of course, the quantum dot in the experiment is not circular symmetric. However, although the asymmetric shape does change the level quantization with respect to $m$ (which then ceases to be a good quantum number), we feel that the general assumption that one state for each $n$ and $s$ is selected by the restricted area of the tunneling current remains valid. This state may still be predominantly $(m=0)$-like with a small contribution of other $m$ states.

Now let us come back to the resonant coupling of the quantum dot states to the bulk DOS. Most likely this coupling broadens the levels. A fit of the $10^4$ individual $dI/dV$ curves from a $(200\ \mathrm{nm})^2$ area shows that a constant FWHM of 3.2 meV for all Gaussian shaped Landau and spin peaks of all curves gives reasonable agreement with the experimental data. It results in an integral intensity error of about 5% for each curve. For one example the fit is shown in Fig. 6(a).

The determined FWHM of 3.2 meV is considerably broader than the energy resolution of the experiment of 0.5 meV. Analysis of the wave functions in Fig. 5(b) reveals that the $(m\neq 0)$ states contribute only about 10% to the tunneling current in the center of the dot. This makes it unlikely that a tunneling into other $m$ states causes the broadening. Thus, we conclude that the coupling to the bulk states changes the width of the levels. The effect is very similar to the broadening of atomic levels of adsorbates by their interaction with surface and bulk states of the sample.[15]

To exclude the possibility that the coupling to the bulk states has an important influence on the energetic positions of the quantum dot states, we want to discuss two experimental observations in more detail.

(1) The presence of ionized dopants changes the potential of the quantum dot and thereby the energy states. We have performed Hartree-Fock calculations with and without a dopant in the center of the dot as shown in Fig. 4(c). We compared the resulting energy shifts of the $(m=0)$ states with a perturbation term $\Delta E_n=\langle\Psi_n|V_{\mathrm{Coul}}|\Psi_n\rangle=V_{\mathrm{Coul}}(\sqrt{n+1}l)$, where $\Psi_n$ describes the wave function corresponding to the $n$th unperturbed Landau state, $V_{\mathrm{Coul}}$ is the screened Coulomb potential of the dopant, and $l$ is the magnetic length.[16] It turns out that the $(n=1)$ and $(n=2)$ states from Hartree-Fock calculations shift by about $2\Delta E_n$ independent of magnetic field. Shifting the dopant away from the center of the dot reduces its influence on the Hartree-Fock energies leading to a continuous change of the energy levels with tip position. In contrast, a dopant embedded in the bulk DOS results in an additional extended state located less than $\Delta E_n$ below the poles of the unperturbed DOS. It exhibits a lateral extension of the order of $d_n=2(\sqrt{n+1}l)$.[17]

To compare these results with the experimental data, Fig. 6(b) shows an area including three dopants visible as bright dots. The dopants are located 5–10 nm below the surface,[18] which is well within the quantum dot area and far away from the 3DEG area [see Fig. 4(a)]. Figures 6(c) and 6(d) show the corresponding experimentally determined $(n=1,s=\downarrow)$

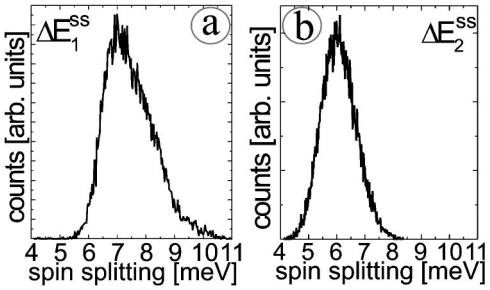


FIG. 7. Histograms of spin splitting energies at $B=6$ T (a) First Landau level; (b) second Landau level. The spin splitting energy $\Delta E_n^{ss}$ is defined as the difference between the two peak energies belonging to the same Landau level $n$: $\Delta E_n^{ss}=E_n^{\uparrow}-E_n^{\downarrow}$. Both histograms are made from the same $10^4$ $dI/dV$ curves covering a $(200\ \text{nm})^2$ area; $V_{\text{stab}}=200$ mV, $I_{\text{stab}}=450$ pA. The spin splitting energy of bulk InAs at 6 T is 5.2 meV.

and $(n=1,s=\uparrow)$ energy states as a function of position at 6 T. The peak energies are very sensitive to position on a length scale well below $d_1=36$ nm. This is expected for the quantum dot levels, since the quantum dot moves with the tip, which slightly changes the total potential of the dot and hence the energy states for each individual $dI/dV$ curve. In addition, the maximum energy shift obtained from Figs. 6(c) and 6(d) is 4 meV, which is indeed twice $V_{\text{Coul}}(\sqrt{n+1}\,l)=2$ meV.[7] Both results, absolute shift and position dependence, are in agreement with the Hartree-Fock calculations of the quantum dot but in disagreement with the expected influence of dopants on the 3DEG. We conclude that the quantization of the bulk bands is of minor importance for the observed energies. Notice that the similar behavior of both spin levels excludes the interpretation that the two levels correspond to a bulk related and a quantum dot related peak. The bulk related peak should be influenced in a different manner by dopants, as discussed above. But more importantly, since the bulklike area is far away from the dopants, the influence of the dopants on the bulk states should be much smaller than its influence on the quantum dot states.

(2) It is well known that quantum dots exhibit other $g$ values than the corresponding bulk material.[13,19] From the Hartree-Fock calculations we can conclude that the major influence for InAs comes from the total spin of the quantum dot, which is the sum of spins of all occupied levels. A high total spin increases the spin splitting of the unoccupied states through the exchange interaction. To estimate this effect, we slightly varied the occupation of the quantum dot as would be expected due to the influence of dopants. It is found that the resulting spin splitting of the $(m=0)$ state can be described by a $g$ value varying between the bulk value ($g\simeq 15$) and twice the bulk value ($g\simeq 30$) for $n=1$. For $n=2$ the maximum value of the spin splitting is slightly lower. Figure 7 shows two histograms of the experimentally observed spin splittings found in a $(200\ \text{nm})^2$ area for the first and second Landau levels. The bulk spin splitting at $B=6$ T is 5.2 meV. Obviously, the experimental results are again in quantitative agreement with the behavior of the calculated states of the quantum dot, but in disagreement with the behavior of the bulk states.

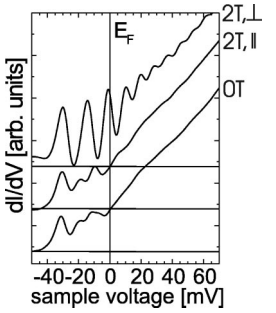


FIG. 8. $dI/dV(V)$ curves obtained with the same microtip on the same sample position at different magnetic fields as indicated; $V_{\text{stab}}=100$ mV, $I_{\text{stab}}=500$ pA. The horizontal lines mark the offset of the curves with respect to each other.

From these two results we conclude that, at least for the quantum dot analyzed in detail, the coupling to the bulk DOS only broadens the detected states of the quantum dot, but does not change their energy considerably. Qualitatively similar results are observed for other tip induced quantum dots.

Finally we would like to show the behavior of $dI/dV$ curves in parallel magnetic field, which is compatible with the above description. Three $dI/dV$ curves obtained with the same tip on the same sample position are shown in Fig. 8. While a field of $B=2$ T perpendicular to the surface results in Landau oscillations, a 2 T field parallel to the surface leaves the $dI/dV$ curve nearly unchanged. In parallel magnetic field, $k_y$ is quantized neither for the quantum dot region nor for the bulk region. Consequently, there are no completely quantized states above $E_{BCBM}$. This seems to prohibit the existence of peaks in the $dI/dV$ curves.

## IV. SUMMARY

In summary, we analyzed the magnetic field induced oscillations observed in $dI/dV$ curves recorded on $n$-InAs(110) and previously attributed to the Landau quantization of the bulk conduction band. It turns out that, although the distance between the peak maxima is compatible with the effective electron mass in InAs, the observed peak energies can only be explained if the tip induced quantum dot is taken into account. The comparison between Hartree-Fock calculations and $dI/dV$ measurements of a particular quantum dot suggests that the tunneling at positive sample voltages proceeds from a nearly featureless tip density of states toward the $(m=0)$ states of different Landau and spin levels of the quantum dot ($m$ is the orbital momentum). These quantum dot states are resonantly coupled to the bulk conduction band of InAs, which leads to a broadening of the levels (FWHM 3 meV), but does not shift the energy states considerably.

## ACKNOWLEDGMENTS

We thank I. Meinel for the help with the Hall measurements. Financial support from SFB 508, WI 1277/15-1 and Graduiertenkolleg ''Physik nanostrukturierter Festkörper'' of the Deutsche Forschungsgemeinschaft is gratefully acknowledged.

[1] K. v. Klitzing *et al.*, Phys. Rev. Lett. **45**, 494 (1980); R.E. Prange and S.M. Girvin, *The Quantum Hall Effect* (Springer, Berlin, 1987).
[2] R. Wiesendanger, *Scanning Probe Microscopy and Spectroscopy* (Cambridge University Press, Cambridge, 1994).
[3] J. Wildoer *et al.*, Phys. Rev. B **55**, 16 013 (1997); R. Dombrowski *et al.*, Appl. Phys. A: Mater. Sci. Process. **66**, 203 (1998).
[4] R. Dombrowski *et al.*, Phys. Rev. B **59**, 8043 (1999).
[5] Chr. Wittneven *et al.*, Rev. Sci. Instrum. **68**, 3806 (1997).
[6] S.D. Jog *et al.*, J. Phys. C **11**, 2763 (1978).
[7] G. Busch and H. Schade, *Vorlesungen über Festkörperphysik* (Birkhäuser, Basel, 1973), pp. 261ff.
[8] M. Morgenstern *et al.*, J. Electron Microsc. Relat. Phenom. **109**, 127 (2000).
[9] U.D. Merkt *et al.*, Phys. Rev. B **35**, 2460 (1987).
[10] V.Y. Aristov *et al.*, Europhys. Lett. **26**, 359 (1994).
[11] V. Ramachandran *et al.*, Phys. Rev. Lett. **82**, 1000 (1999).
[12] V. Gudmundsson *et al.*, Phys. Rev. B **52**, 16 744 (1995); A. Manolescu *et al.*, *ibid.* **59**, 5426 (1999).
[13] V. Gudmundsson *et al.*, Phys. Rev. B **49**, 13 712 (1994).
[14] J. Wildoer *et al.*, Phys. Rev. B **53**, 10 695 (1996).
[15] D.M. Eigler *et al.*, Phys. Rev. Lett. **66**, 1189 (1991).
[16] D. Gekhtman *et al.*, Phys. Rev. B **54**, 2756 (1996).
[17] O.P. Gupta *et al.*, Phys. Rev. B **25**, 1101 (1982).
[18] Chr. Wittneven *et al.*, Phys. Rev. Lett. **81**, 5616 (1998).
[19] V. Gudmundsson *et al.*, Phys. Scr. **T54**, 92 (1994).